World Academy of Science, Engineering and Technology
International Journal of Materials and Metallurgical Engineering
Vol:3, No:10, 2009

The temperature range in the simulation of residual stress and hot tearing during investment casting

Saeid Norouzi, Ali Shams, Hassan Farhangi, Alireza Darvish

***Abstract*—**Hot tear cracking and residual stress are two different consequences of thermal stress both of which can be considered as casting problem. The purpose of the present study is simulation of the effect of casting shape characteristic on hot tearing and residual stress. This study shows that the temperature range for simulation of hot tearing and residual stress are different. In this study, in order to study the development of thermal stress and to predict the hot tearing and residual stress of shaped casting, MAGMASOFT simulation program was used. The strategy of this research was the prediction of hot tear location using pinpointing hot spot and thermal stress concentration zones. The results shows that existing of stress concentration zone increases the hot tearing probability and consequently reduces the amount of remaining residual stress in casting parts.

***Keyword*—**Hot tearing, Residual stress, Simulation, Investment casting.

I. Introduction

A. Numerical simulation

NOWADAYS, simulation is widely used as a part of manufacturing processes. The use of numerical simulation leads to increase in efficiency and decrease in experimental trial and error in the casting process. The numerical simulation of thermal stress during solidification is an important way to predict hot tearing, cold crack, residual stress, and distortion.

A reliable and useful simulation must be relied on the experimental background, and the strong theory-and-approach. Regarding the simulation of hot tearing, several approaches have been suggested. They are used to explain and to predict occurrence of hot tear from different points of view. For example, one approach is metallurgical approach in which metallurgical characteristics such as freezing range [1-3], solidification time [4], shrinkage porosity [4], segregation and chemical composition [5, 6], and feeding efficiency in order to compensate shrinkage and deformation [7, 8] are taken into account. The second approach, which is a mechanical approach, assumes that failure occurs at a critical stress/strain level. In this approach some criteria such as strain rate and total strain [9] are used for the prediction of hot tearing.

On the basis of the mentioned approaches, several models have been proposed. For instance, a rheological modeling was used by Liu et al. [10] to model the stress of quasi-solid zone with the aim of predicting hot tearing.

Saeid .Norouzi: MAPNA GROUP, MEEMCo., Iran; (s_norouzi@mapnaequipment.com)
S. Norouzi, Ali Shams & H. Farhangi: School of Metallurgy and Materials Engineering, University of Tehran, Iran; (hfarhangi@ut.ac.ir)
A. Shams & A. Darvish: Badr System Co.:(a.shams@badrsystem.com)

They explained a criterion based on visco-plastic strain for determining the hot tearing tendency. They also used thermo-elasto-plastic model to simulate the behavior of material in the period after solidification in order to predict residual stress.

Moreover, a physical model based on a mass balance was developed by Monroe et al. [11] to find additional porosity formation and initiation sites for hot cracking in castings. Based on a mass balance performed over the liquid and solid phases, a criterion for the appearance of hot tears in metallic alloys has been proposed by Rappaz et al. [5].

The purpose of the present study is simulation of the effect of casting shape characteristic on hot tearing and residual stress and finding the suitable temperature ranges and boundary conditions for simulation.

B. Thermal stress during casting

Thermal contraction associated with decreasing temperature and changing the state of material exerts thermal stress during casting. Thermal stress involves different consequences such as distortion, crack, hot tear, and residual stress. All of them have significant effect on the quality of casting products.

Hot tearing or solidification cracking is one of the major discontinuities in casting process. Hot tear occurs at high temperature during latter stages of solidification in which there is only a small fraction of remaining liquid in the interdendritic region. Hot tear formation is caused by the inability of the material to withstand the existing thermal stress/strain in the semi-solid state. Thermal stress is mainly induced by the uneven thermal contraction of castings and hindered contraction by mold, core, or casting components [12]. The formation of hot tear is also linked to the lack of feeding in the mushy zone, but only for specific regions where the dendritic network is submitted to shear or tensile stresses [6].

The thermal gradient is the main reason why thermal stress is generated throughout the casting body. The material temperature and semi-solid specification changes during solidification. At special temperature range which is called *coherency temperature*, the dendrite network starts to coalesce. In this case, the material can sustain and transmit the stress. Above this temperature, the percentage of liquid at the coexistence of solid and liquid is quite high. Thus, the dendrite network cannot coalesce completely. At some locations, the dendrite arms start to pull apart; while the fresh melt can compensate for this by flowing in and healing the tear. Nonetheless, deep in the mushy zone where the permeability of the mush is very small, an opening of the non-coherent dendritic network caused by tensile deformation cannot be compensated for by the liquid, and hence the hot tear forms [5].

Another phenomenon which has a prominent effect on the soundness of casting is residual stress. Residual stress in cast components is elastic stress generated up to room temperature due to non-uniform expansion and contraction rates from point to point within the casting [13–15].

II. Experimental

A. Casting process

Two different 3-bar sample castings were used in this research. The difference between the two models arose from their corner geometry as shown in Figure 1. The investment casting process consisting of several steps was employed to produce test specimens. A special wax was injected into the die to make the primary patterns, which were then subjected to a number of alternate exposures of ceramic slurry and coarse ceramic stucco in order to build a green shell of suitable thickness. The nickel-base superalloy IN738LC with the chemical composition shown in Table1 was poured into the preheated mold after removing the wax, and drying and baking the ceramic shell mold. Casting process was carried out using a vacuum induction melting furnace. The casting conditions are listed in Table2.

B. Residual strain measurement method

The magnitude of residual stress in the central bar of the respective sample castings was evaluated using cutting technique. Two markings were inscribed on the central bar prior to cutting process which was done using wire cut machine. The spacing of the markings was set at 200mm. The increase in the spacing of the markings was then measured using a coordinate measurement machine.

C. Finding coherency temperature

The setup shown in Figure 2 was prepared to find the coherency temperature. This apparatus is a modified version of which designed by Wang *et al* [16] to assess the thermal stress during solidification of a magnesium alloy. Embedded thermocouple in the middle of the part records the cooling curve (temperature versus time) and the indicator located at the end of the mold, shows the temperature that semi-solid state starts to transmit stress and likewise indicates the commence of the thermal strain.

Three thermocouples, according to Figure 3, were embedded in the Central Bar (CB), Side Bar (SB), and Hot Spot (HS) of the model to record the thermal history and cooling curves corresponding to these three points.

TABLE I
CHEMICAL COMPOSITION (WT.%)

C	Cr	Co	Mo	W	Nb	Ta	Ti	Al	B	Zr	Ni
0.09	16	8.5	1.7	2.5	0.8	1.7	3.5	3.5	0.01	0.1	Bal

TABLE II
CASTING CONDITIONS

Pressure	Preheat Temp.	Pouring Temp.
$3*10^{-3}$mbar	1050°C	1450°C

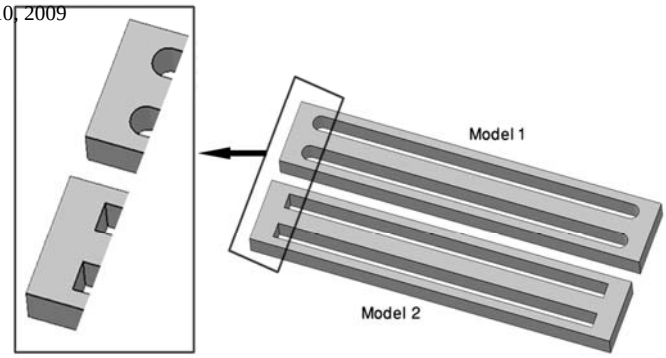

Fig.1. Selected models for evaluating residual stress and hot tear.

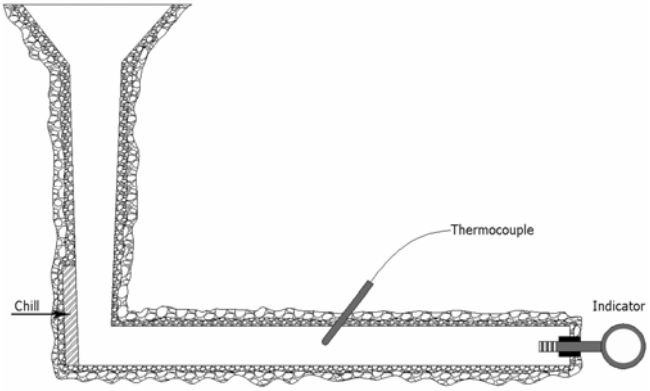

Fig. 2. Apparatus to measure coherency temperature.

III. Results and Discussion

A. Thermal stress

Special geometry of the selected model encourages hot tearing at the hot spot during contraction of the inner bar while two outer bars have been solidified and hot spot is in its semi-solid state. Thermal contraction causes tensile stress in the central bar and compressive stress in the outer bars. After pouring the melt, the lighter sidebars begin to solidify and contract first while the heavier central bar is still liquid and contracts freely under the resulted compressive loads. Solidification of the central bar starts when the sidebars have practically solidified. Therefore, contraction of central bar induces tensile stress, which is concentrated in the hot spot that is in the latest stage of solidification. This uneven thermal gradient caused internal stress. Yubo *et al* [17] have explained the effect of uniform temperature distribution on the decreasing the internal stress. The temperature difference throughout the casting part causes uneven thermo-mechanical behavior which is the main reason of thermal stress.

It is crucial to have estimation about a very important parameter, the coherency temperature, to evaluate the thermo-mechanical behavior in the semi-solid state. The coherency temperature is defined as a temperature that dendrite branches start to make solid bridge and transmit the stress. The coherency temperature for this alloy has been resulted about $1270^{\circ C}$ using the apparatus shown in Figure 2. The coherency temperature is located between liquidus and solidus temperatures and divides freezing range into two parts which are thermo-mechanically different.

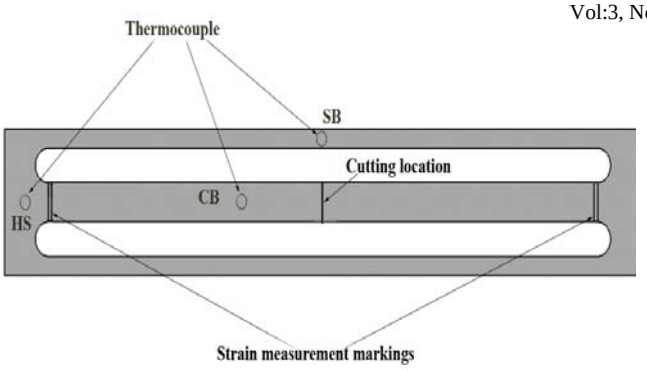

Fig. 3. The location of thermocouple and markings

Figure 4 demonstrates the cooling curves extracted from embedded thermocouples in the central bar, sidebar and hot spot. The difference between cooling rates of three discrete regions is obvious; the sidebars and hot spot have the highest and the lowest cooling rate, respectively. The critical temperature range for hot tearing to occur corresponds to the lower end of freezing range, where the solid fraction is high enough to prevent feeding and to allow the development of stress in the presence of thin interdenderitic liquid layers. In the microstructural terms, this situation occurs when the secondary dendrite arms begin to contact each other and bonds begin to form between them [3]. The interval between coherency temperature and solidus temperature provides the suitable condition for formation of hot tear cracking. In this interval there is an important temperature range, Zero Ductility Range, in which a thin inter-dendritic liquid layer causes significant reduction in strength and promotes liquid embrittlement. While the hot spot is reaching to zero ductility temperature, the central bar is in the solid state and inducing tensile stress due to contraction. From this point, the tensile stress in the central bar, consequently in the hot spot, and compressive stress in the sidebars start to accumulate.

Tensile stress is the first requirement for the occurrence of hot tear. Another requirement is presence of the thin liquid layer in the interdenderitic regions. So, the solid fraction is a necessary criterion to evaluate the situation. The solid fraction of hot spot corresponding to the zero ductility temperature is more than 95% in which feeding the hot spot is impossible, while there are thin liquid layers between dendrite arms. Wang [18] observed that hot tear occurred under a small strain when the interdentritic liquid film was thin enough to resist feeding of the surrounding liquid through the dendrite arms.

The thermo-mechanical behavior of the solidifying material after coherency temperature determines whether or not hot tear occurs. After this temperature semi-solid state acquires strength through coalescence and bridging of dendrites, which it has two consequences; on one hand, the stress can be transferred through the semi-solid mush, and the force of thermal contraction of the central bar can be translated into tensile stress in the hot spot, which it increases the hot tear possibility. On the other hand, the build-up of strength can be faster than the build-up of stress, and at a certain (high) solid fraction, the mush would be strong enough to withstand the existing stress [9], in this case the hot tear probability decreases.

In other words, there is a competition between increasing thermal stress/strain and increasing the strength of material during solidification. Increasing the thermal stress, resulted from thermal contraction, and increasing the strength of material, resulted from decreasing temperature, happen simultaneously.

B. Thermal stress components

All generated stress, due to thermal contraction, does not take part in the formation of hot tear since some part of solidification stress is partially released. So, the generated thermal stress during solidification is divided into several parts:

$$\sigma_{th} = \sigma_{HT} + \sigma_{SC} + \sigma_{DS} + \sigma_{RS} \quad (1)$$

Where σ_{th} thermal stress, σ_{HT} stress released by hot tear, σ_{SC} solid creep stress, σ_{DS} deformation/distortion stress, and σ_{RS} residual stress remaining in the bulk. In other words, σ_{th} has two main parts. One part remaining in the bulk as a residual stress, and second part released by stress relaxation mechanisms such as creep, rearrangement of grains, initiation of cracks, and distortion.

The amount of each part depends on casting condition and casting design geometry. In model 1, the amount of residual stress is higher than that of in model 2 due to releasing some part of stress by opening up the hot tear crack in the model 2. Table 3 shows the amount of relaxed strain resulted from cutting technique. This strain is in direct relation with relaxed residual stress. In some specimens there are no any hot tear, since hot tearing occurs in a material whenever the strain caused by shrinkage during solidification cannot be accommodated by elastic and plastic deformation of the alloy [3].

The amount of thermal stress is related to the amount of solidification contraction. The following equation explains the overall contraction in the several steps during solidification;

$$\varepsilon_{total} = \int_{T_{pour.}}^{T_{liq.}} (\beta^{\frac{1}{3}} + \alpha_l(T))dT + \int_{T_{liq.}}^{T_{coh}} [(\beta^{\frac{1}{3}} + \alpha_l(T)) f_l(T) + \alpha_s(T) f_s(T)]dT + \int_{T_{Coh}}^{T_{sol.}} f_s(T)\alpha_s(T)dT + \int_{T_{Sol.}}^{T_{room}} \alpha_s(T)dT \quad (2)$$

Where α_s and α_l are the thermal expansion coefficient of solid and liquid alloy, respectively. And, β is the volume shrinkage coefficient of liquid during solidification. f_s and f_l are solid and liquid fraction, respectively. The *(T)* indicates that α and fraction solid have non-linear characteristic and change by changing the material temperature. Although the total contraction comprises four terms, explained in the right-hand side of the equation 2, only the small amount of it contribute in generation of thermal stress which is responsible for hot tearing occurrence. This limited range corresponds to the contraction of central bar while the hot

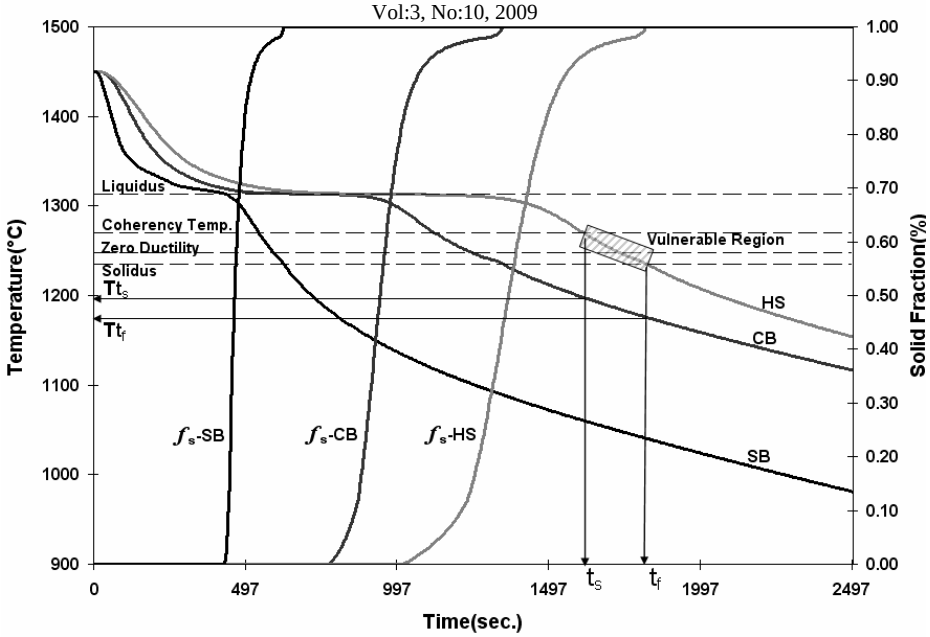

Fig. 4. Cooling (Time-Temperature) curves and solid fraction curves related to the three distinct regions of selected model; SB: Side Bars, CB: Central Bar, HS: Hot Spot. Hatched rectangle shows vulnerable region of hot spot. Illustration also shows four important temperatures; liquidus temperature: 1313°C, coherency temperature: 1270°C, zero ductility: 1255°C, solidus: 1235°C.

spot is in the critical temperature range which is shown in Figure 4. t_s and t_f are start and finish time of critical range, respectively. Thermo-mechanical behavior when hot spot is in this range affects hot tearing phenomenon. If the tensile stress at a temperature near the solidus exceeds the strength of the alloy at the corresponding temperature, hot crack will be generated [17]. So, the effective contraction can be written as following equation;

$$\Delta_{\text{e-hot tear}} = \int_{T_{t_s}}^{T_{t_f}} f_s(T)\alpha_s(T)dT \tag{3}$$

Where, Δ_e is the effective contraction of central bar on hot tear. T_{ts} and T_{tf} are the central bar temperatures at which hot spot is in its coherency temperature and solidus temperature, respectively. It indicates that the longer freezing range, the higher hot tear susceptibility, since for long freezing range alloys the vulnerable temperature range is wider, and hot spot remains in such condition for a longer time. Phillion [18] explained the effect of freezing rang of a binary alloy on hot tearing and showed that alloys with longer freezing rang have higher hot tear susceptibility.

On the other hand, residual stress is measured and evaluated in the room-temperature, and it can be considered only after completion of contraction. And given that contraction in liquid state and higher than coherency temperature does not contribute in building up the residual stress, the amount of thermal stress which has effect on magnitude of residual stress can be expressed as following equation;

$$\Delta_{\text{e-R.S}} = \int_{T_{Coh.}}^{T_{sol.}} f_s(T)\alpha_s(T)dT + \int_{T_{Sol.}}^{T_{room}} \alpha_s(T)dT \tag{4}$$

Where $\Delta_{\text{e-R.S}}$ is the effective contraction of central bar having effect on residual stress. Comparison between Eq. 2 and 3 indicates that, if hot tear occurs, the significant amount of stress, generated by thermal contraction, will be released. Hence, the amount of final residual stress/strain will decrease.

The volume solid fraction which has been used in the previous equation strongly depends on temperature. During solidification, dendrite arms continue to coarsen through various ripening mechanisms and intergranular regions decrease in size as the volume fraction of solid increases. The solid fraction is determined as below;

$$f_s(T) = \frac{T_l - T}{T_l - T_s} \tag{5}$$

And the changing rate of f_s in the solidification time according to cooling curve is derived by following equation;

$$\frac{\partial f_s}{\partial t} = \frac{\partial f_s}{\partial T}\frac{\partial T}{\partial t} \tag{6}$$

C. Hot tear surface characteristics

Figure 5 shows a hot tear fracture surface. The figure shows the separated solid bridges and free dendrites some of which are broken. Also the last solidified intergranular layer and an interdenderitic crack are visible in this picture. The last stage of hot tearing can be explained by the transition from a mushy state, where almost all the solidifying grains are separated by liquid films so that the mechanical properties are mostly controlled by the liquid phase ($f_s \leq 0.95$), to a state where the solid skeleton is significantly connected. The solid fraction of 0.95 at which this transition occurs corresponds to the so-called fraction of coalescence found in the literature [19].

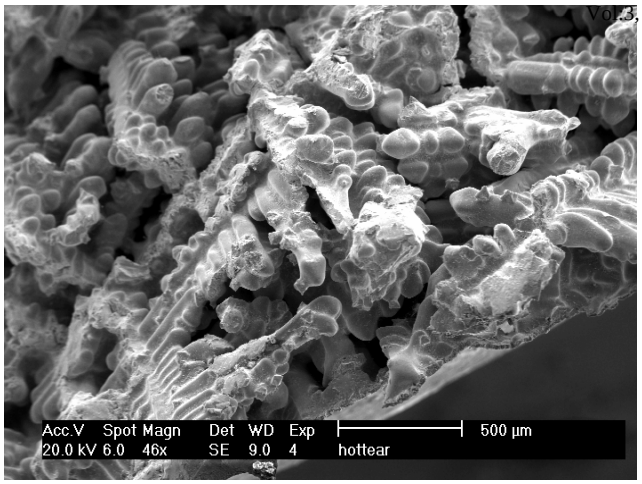

Fig. 5. Hot tear surface: consist of brittle dendritic surface, last solidified eutectic phase, interdendritic tear, and separated solid bridges.

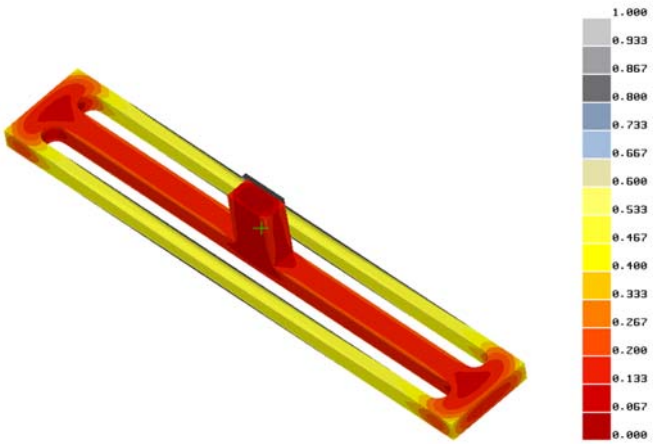

Fig. 6. Hot spot localization through solid fraction profile.

IV. Casting Simulation

Two software, MAGMASOFT and ProCAST, were used to simulate the casting process. The casting geometry was directly input into the simulation software through the built-in STL interface. Some of the thermal and physical properties of the casting alloy and ceramic shell mold were found in the software database, and some of them extracted from experimental results. In this research, simulation was based on three main steps which are required for hot tear to happen:

First, finding the temperature distribution in each time step and pinpointing the hot spot.

Second, evaluating solid fraction result to find the region which is cut off from feeder and fresh melt to compensate solidification shrinkage.

Third, simulation of thermal stress distribution to specify the stress concentration region.

Development of thermal stress is closely related to the cooling condition of casting, and therefore, the numerical simulation of thermal stress must be based on the thermal analysis [12]. Figure 6 shows the fraction solid as a result of thermal distribution analysis. According to this figure, it can be seen that the hot spot region are located in the two ends of central bar.

During the solidification simulation, the solid fraction was calculated and used to predict shrinkage locations. Solid fraction result indicates that the relation from hot spot to feeder was cut off. This result also demonstrates the last solidifying region is susceptible to hot tear on the ground that the rate of build-up of thermal stress becomes more than the rate of strengthening of alloy due to cooling down.

Figure 6 illustrates the location of latter solidified liquid. In the model of choice, because of cutting of the relation between hot spot and feeder, the fresh melt could not compensate increasing volume due to opening hot tear crack.

According to Figure 4, for prediction of hot tear, the thermo-mechanical behavior of model in the critical range, between t_s and t_f, must be considered. According to Eq. 3, there is a vulnerable range in which hot tear occurs, hence the simulation to predict hot tearing must be done in this range. The lower integration limit is the time at which the local temperature reaches the coherency temperature, i.e., $T < T_{coherent}$, regardless of the availability of liquid feeding. In the models of choice because of cutting off feeder and hot spot, subsequently lack of fresh melt, healing of hot tearing crack is very hard.

Figure 4 and 6 indicate that while the outer bars were contracting in solid state, the hot spot was in semi-solid state, which increases hot tear susceptibility. Figure 7 shows the hot tear susceptibility at different parts of casting. It is clear that the hot tear susceptibility at hot spot is more than that of at other sections. In this special model, besides the thermal gradient, the corner geometry has a direct effect on hot tear probability.

To further demonstrate the importance of corner shape effect on the present hot tear prediction, two simulations corresponding to the model 1 and 2 were performed. The simulation results related to the models 1 and 2 indicate that concentration of thermal stress and strain in the model 2 increases the hot tear susceptibility. However, in the model 1 low stress concentration decreases hot tear probability and increases the amount of residual stress in the part after completion of solidification. The difference between distributions of thermal strain corresponding to two models with different corner geometry is shown in Figure8.

If the strains are much larger than what the material can accommodate by elastic deformation, strains will result in flow of the liquid or plastic deformation of the solid, which may induce the formation of hot tears [11]. Eq. 1 explained that thermal stress is divided into several parts; therefore, If the amount of thermal stress is assumed constant, in the case that there is not any stress relaxation due to opening up the hot tear, the amount of residual stress will be increased. Figure 9 demonstrates the residual strain distribution in model 1 after completion of solidification. Comparison simulated results and experimental results, showed in Table 2, demonstrate a good agreement between simulation and experimental results.

TABLE III
THE AMOUNT OF RESIDUAL STRAIN RELAXED AFTER CUTTING*.

Model type	Residual strain (* 10^{-3})
Model 1	4±1.2
Model 2	1.5±0.5

*authors have explained the results of residual strain elsewhere extensively [14].

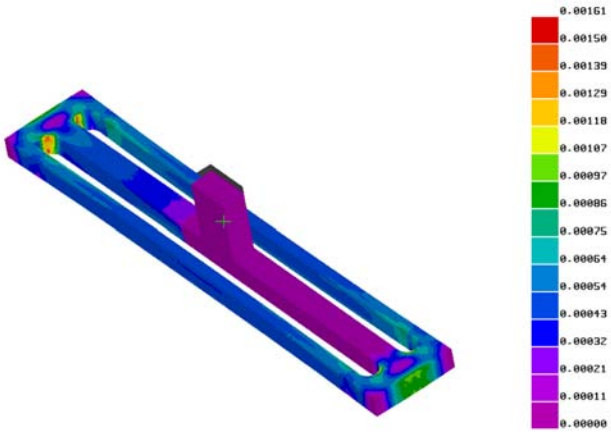

Fig. 7. Hot tear susceptibility.

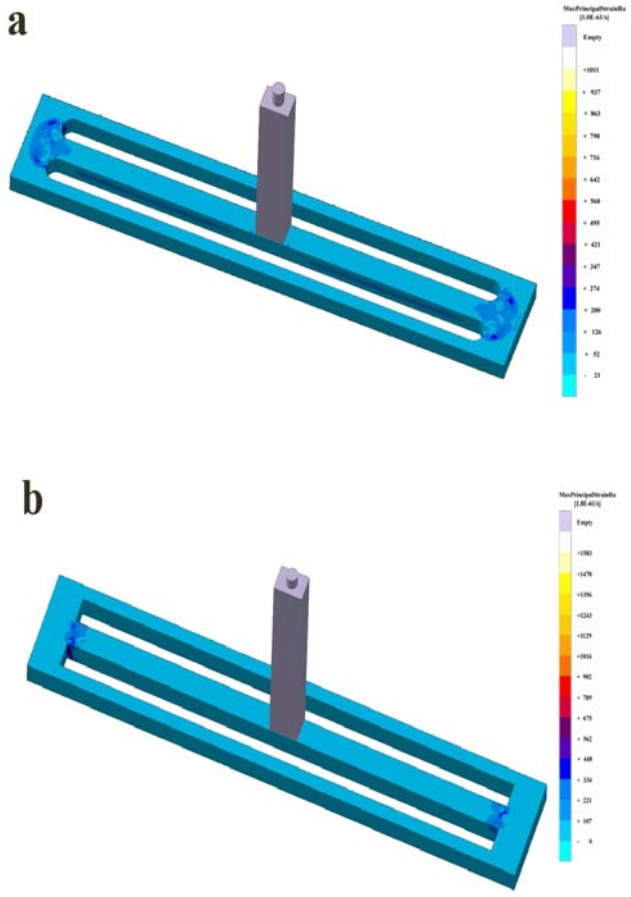

Fig. 8 The difference between strain concentration in two selected models due to the effect corner shape; a) model 1, b) model 2.

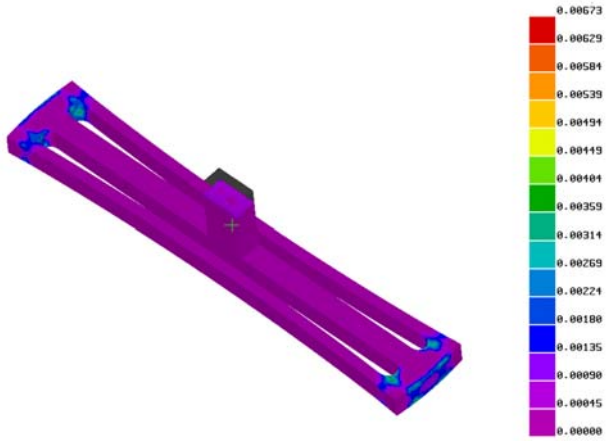

Fig. 9. Residual strain pattern.

V. CONCLUSION

1- Existing of stress concentration zone, which is related to the casting geometry, increases hot tearing probability and consequently reduces the amount of remaining residual stress in casting parts.

2- There is a vulnerable range in which hot tear may occur, hence the simulation to predict hot tearing must be done in this range. This temperature range is between coherency temperature and solidus temperature.

3- Residual stress is a room-temperature phenomenon; so, the temperature range for simulating residual stress must be between coherency temperature and room temperature.

ACKNOWLEDGMENT

Authors would like to thank Mr. Javadi, Mr. Shafaati, and Mrs. Karimi for their precious help. This project was financially supported by MAPNA GROUP-MEEMCo.

REFERENCES

[1] Jason Mitchell, "Determination of strain during hot tearing by image correlation," *Materials Engineering Research Colloquium,* December 2, 2005.

[2] D.G. Eskin, Suyitno, and L. Katgerman, "Mechanical properties in the semi-solid state and hot tearing of aluminium alloys," *Progress in Materials Science*, vol. 49, pp. 629–711, 2004.

[3] J. Zhang and R.F. Singer, "Hot tearing of nickel-based superalloys during directional solidification," *Acta Materialia*, vol. 50, pp. 1869–1879, 2002.

[4] A.B. Phillion,a S.L. Cockcroft, and P.D. Lee, "X-ray micro-tomographic observations of hot tear damage in an Al–Mg commercial alloy," *Scripta Materialia*, vol. 55, pp. 489–492, 2006.

[5] M. Rappaz, J.-M. Drezet, and M. Gremaud, "A New Hot-Tearing Criterion," *Met. and Mat Trans. A*, vol. 30A, pp. 449, February 1999.

[6] Y. Wang , Q. Wang, G. Wu, Y. Zhu, and W. Ding, "Hot-tearing susceptibility of Mg–9Al–xZn alloy," *Materials Letters*, vol.57, pp. 929– 934, 2002.

[7] M. Easton, H. Wang, J. Grandfield, D. St. John, and E. Sweet, "An Analysis of the Effect of Grain Refinement on the Hot Tearing of Aluminum Alloys," Materials forum, vol. 28, Institute of Materials Engineering Australasia Ltd, Published 2004.

[8] M. Blair, R. Monroe, C. Beckermann, R. Hardin, K. Carlson, and C. Monroe, "Predicting the Occurrence and Effects of Defects in Castings," JOM, pp.29-34, May 2005.

[9] Suyitno, D.G. Eskin, and L. Katgerman, "Structure observations related to hot tearing of Al–Cu billets produced by direct-chill casting," *Materials Science and Engineering A*, vol.420, pp. 1–7, 2006.

[10] B. C. Liu, J. W. Kang, and S. M. Xiong, "A study on the numerical simulation of thermal stress during the solidification of shaped

castings," *Science and Technology of Advanced materials*, vol. 2, 157-164, 2001.
[11] C. Monroe and C. Beckermann, "Development of a hot tear indicator for steel castings," *Materials Science and Engineering A*, vol. 413-414, pp. 30–36, 2005.
[12] H. Farhangi, S. Norouzi, and M. Nili-Ahmadabadi, "Effects of casting process variables on the residual stress in Ni-base superalloys," *Journal of Materials Processing Technology*, vol. 153–154, pp. 209–212, 2004.
[13] J. Withers and H.K.D.H. Bhadeshia, "Residual stress. Part 2. Nature and origins," *Mater. Sci. Technol.*, vol.17, pp.366–375, 2001.
[14] E. Macherauch, "Introduction to residual stress," *Exp. Mech.*, vol. 25, pp. 1–35, 1984.
[15] C.H. Reese and K.B. Rundman, "Residual stress in gray cast iron brake rotors," *AFS Trans.*, vol. 115, pp. 175–181, 1997.
[16] Y. Wang, B. Sun, Q. Wang, Y. Zhu, and W. Ding, "An understanding of the hot tearing mechanism in AZ91 magnesium alloy," *Materials Letters*, vol. 53, pp. 35–39, 2002.
[17] Z. Yubo, C. Jianzhong, Z. Zhihao, Z. Haitao, and Q. Ke, "Effect of low frequency electromagnetic field on casting crack during DC casting super-high strength aluminum alloy ingots," *Materials Science and Engineering A*, vol. 406, pp. 286–292, 2005.
[18] A.B. Phillion,a S.L. Cockcroft, and P.D. Lee, "X-ray micro-tomographic observations of hot tear damage in an Al–Mg commercial alloy," *Scripta Materialia*, pp. 55, pp. 489–492, 2006.
[19] D. Fabre`gue, A. Deschamps, M. Suery, and J.M. Drezet, "Non-isothermal tensile tests during solidification of Al–Mg–Si–Cu alloys: Mechanical properties in relation to the phenomenon of hot tearing," *Acta Materialia*, vol. 54, pp. 5209–5220, 2006.